Supplementary Information

Porous confinement: Stable and full exposure of Ru nanoparticles towards efficient electrocatalytic hydrogen evolution

Qingying Qiao, Leyi Zhang, Jinping Zhang, Wenqing Zhang, Han Lu, Shaohan Zhu, Fei Li, Fenghua Zhang,* Wei Wei* and Yongya Zhang**

Experimental

1. Materials

High-purity argon (Ar) and 5% H_2/Ar mixed gases were supplied by *Comfort Gas Co., Ltd*. Activated carbon, 2,2'-azobis(2-methylpropionamidine) dihydrochloride (AIBA) and ruthenium(III) chloride hydrate ($RuCl_3 \cdot xH_2O$) were purchased from *J&K*. 1-vinylimidazole, 1,2-dibromoethane and potassium hydroxide (KOH) were acquired from *Macklin Inc*. Commercial Pt/C catalyst (20 wt% Pt) was purchased from *Alfa Aesar*. 1-vinyl-3-butylimidazolium bromide (VBImBr) was supplied by the Centre for Green Chemistry and Catalysis, *LICP*, *CAS*. All experimental water was obtained via an ultrapure water purification system. Other chemicals and solvents were obtained from local suppliers and used as received.

2. Preparation

2.1. Synthesis of ionic crosslinker N, N-ethylene bisvinylimidazolium bromide (EBVImBr)

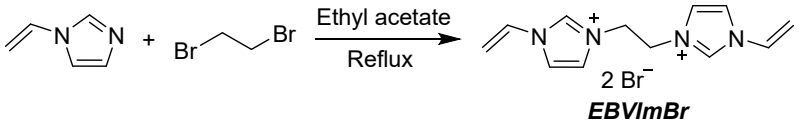

EBVImBr

1-Vinylimidazole (1.882 g, 20 mmol) was dissolved in 10 mL ethyl acetate in a 100 mL round-bottom flask. Subsequently, 1,2-dibromoethane (1.879 g, 10 mmol) was dissolved in another 10 mL ethyl acetate and added to the flask dropwise. The obtained mixture was stirred and heated in an oil bath at 80 °C for 12 h, leading to the precipitation of a large amount of white powder. After the solution was cooled to room temperature, the liquid phase was decanted. The resulting white powder was washed with ethyl acetate three times to remove residual impurities, dried by rotary evaporation, and further vacuum-dried to constant weight. The white powder solid of 3.651g was obtained in a 97% yield.

^{1}H NMR (400 MHz, D_2O, TMS) δ (ppm): 9.11 (s, 2H), 7.82 (s, 2H), 7.54 (s, 2H), 7.10 (dd, J = 16.0, 8.0 Hz, 2H), 6.10 (dd, J = 8.0, 4.0 Hz, 2H), 5.51 (dd, J = 8.0, 4.0 Hz, 2H), 4.81 (s, 4H); ^{13}C NMR (100 MHz, D_2O, TMS) δ (ppm): 135.85, 127.94, 122.53, 120.95, 111.56, 59.26.

2.2. Synthesis of RuO_2/PIL

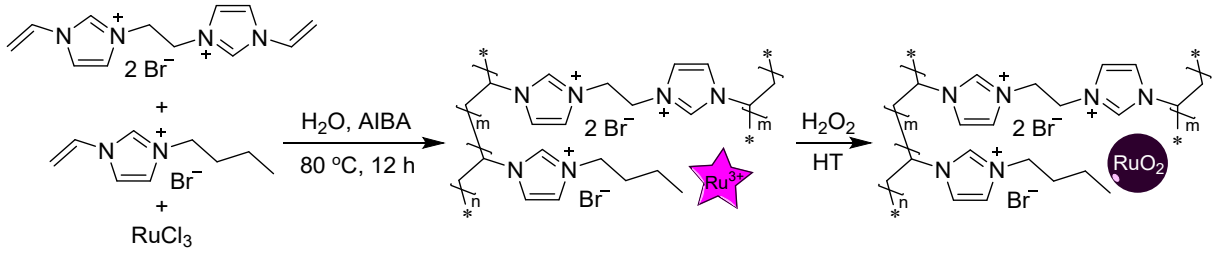

VBImBr (0.752 g, 3.25 mmol) and EBVImBr (0.752 g, 2 mmol)with a mass ratio of 1:1 were accurately weighed into a 50 mL round-bottom flask. 2 mL of ultrapure water was added, and the mixture was sonicated for 15 min to form a clear and transparent solution. Then, $RuCl_3 \cdot xH_2O$ (50 mg, with Ru of approximately 20 mg) was added to the above mixed solution and stirred at room temperature for 2 h to form a homogeneous dispersion. Subsequently, 150 mg of AIBA was added and the mixture was then heated and stirred in an oil bath at 80 °C for 12 h. After polymerization, brown solid was obtained. To convert the Ru species to RuO_2, hydrogen peroxide (H_2O_2, 30 wt%) was slowly added to the solid particles, which were then transferred to a hydrothermal autoclave and heated at 200 °C for 3 h to ensure complete oxidation to obtain dark browm solid RuO_2/PIL.

2.3. Synthesis of Ru/PIL-PC-T

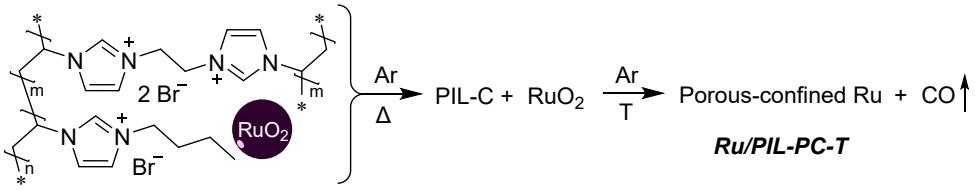

The as-prepared RuO_2/PIL composite was divided into four equal parts and pyrolyzed at 500 °C, 600 °C, 700 °C, 800 °C, respectively. Calcination was performed under Ar atmosphere with a heating rate of 2 °C min^{-1} and a holding time of 2 h. Finally, the Ru/PIL-PC-T catalysts were obtained, where T represents the pyrolysis temperature.

2.4. Synthesis of PILC-700

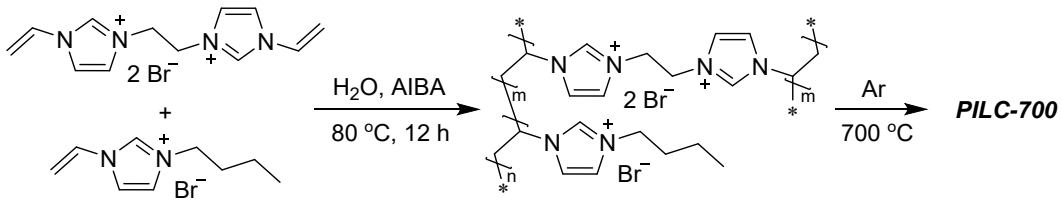

VBImBr (0.752 g, 3.25 mmol) and EBVImBr (0.752 g, 2 mmol) with a mass ratio of 1:1 were accurately weighed into a 50 mL round-bottom flask. 2 mL of ultrapure water was added, and

the mixture was sonicated for 15 min to form a clear and transparent solution. Then, 150 mg of AIBA was added and the mixture was heated and stirred in an oil bath at at 80 °C for 12 h. After polymerization, white solid was obtained which was then pyrolyzed at 700 °C under Ar atmosphere with a heating rate of 2 °C min^{-1} and a holding time of 2 h to acquire black powder PILC-700.

2.5. Synthesis of Ru/r-PILC

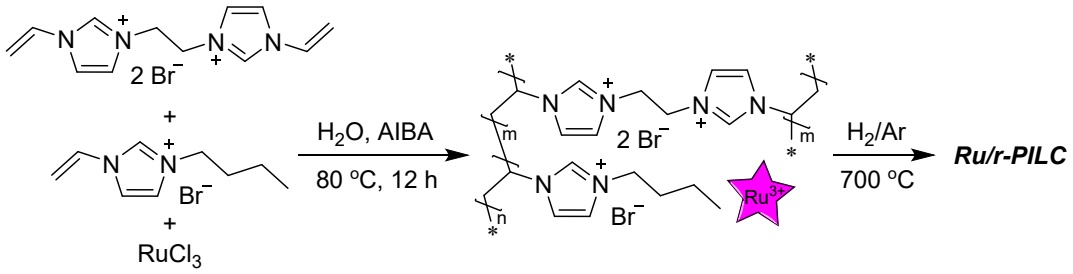

VBImBr (0.188 g, 0.8 mmol) and EBVImBr (0.188 g, 0.5 mmol) with a mass ratio of 1:1 were accurately weighed into a 50 mL round-bottom flask. 0.5 mL of ultrapure water and 1 mL of ethanol was added, and the mixture was sonicated to form a homogeneous solution. Then, $RuCl_3 \cdot xH_2O$ (12 mg, with Ru of approximately 5 mg) was added to the above mixed solution and stirred at room temperature for 2 h to form a homogeneous dispersion. Subsequently, 40 mg of AIBA was added and the mixture was then heated and stirred in an oil bath at 80 °C for 12 h. After polymerization, brown solid was obtained which was then pyrolyzed at 700 °C under H_2/Ar reduced atmosphere with a heating rate of 2 °C min^{-1} and a holding time of 2 h to acquire black powder Ru/r-PILC.

2.6. Synthesis of Ru@AC

Activated carbon (75.24 mg) was added in a 50 mL round-bottom flask, then $RuCl_3 \cdot xH_2O$ (12 mg, with Ru of approximately 5 mg) was dissolved in 5 mL of ultrapure water and added dropwise. The mixture was sonicated for 3 h to facilitate the impregnation and dispersion of Ru precursors on activated carbon surface. Subsequently, the mixture was stirred at room temperature for 48 h. The obtained black suspension was rapidly cooled with liquid nitrogen and then vacuum-dried for another 48 h to obtain black particles. After annealed at 700 °C under Ar atmosphere with a heating rate of 2 °C min^{-1} and a holding time of 2 h, the product Ru@AC was obtained.

3. Instruments and Characterizations

Transmission Electron Microscopy (TEM) analysis was performed on a JEOL JEM-F200 microscope (JEOL Ltd., Japan) to characterize the morphology and size of the as-prepared samples. N_2 adsorption-desorption measurements were conducted at 77 K using a Micromeritics ASAP 2460 analyzer (Micromeritics Instrument Corp., USA) to evaluate the specific surface area and porous structure of the catalysts. Powder X-ray Diffraction (XRD) patterns were collected on a Bruker D8 Discover X-ray diffractometer (Bruker Corp., Germany) equipped with a Cu Kα radiation source (λ = 1.5406 Å). The scanning was performed from 5° to 90° at a rate of 5°/min to identify the crystalline phases of the catalysts. Raman spectra were recorded using a Zolix Raman spectrometer (Zolix Instruments Co., Ltd., China) with a 532 nm excitation wavelength (employing a helium-cadmium laser source and a CCD detector) to investigate the graphitization degree and defect density of the carbon supports. X-ray Photoelectron Spectroscopy (XPS) analysis was carried out on a Thermo Fisher Scientific K-Alpha spectrometer (Thermo Fisher Scientific Inc., USA) with a monochromatic Al Kα X-ray source (hv = 1486.6 eV). All binding energy data were calibrated against the C 1s peak at 284.8 eV. The XPS spectra were fitted and analyzed using Avantage software to determine the elemental composition and chemical valence states of metal atoms in the catalysts. Thermogravimetric (TG) analysis was carried out using a NETZSCH STA449 F3 Jupiter instrument (Netzsch, Germany) at a heating rate of 10 °C /min with a sample weight of approximately 5-8 mg in air atmosphere.

4. Electrochemical Measurements

The electrocatalytic hydrogen evolution reaction (HER) performance was evaluated using a standard three-electrode configuration on a CHI-760E electrochemical workstation. A platinum plate (10 mm × 10 mm) and a HgO/Hg electrode (filled with 1.0 M KOH) served as the counter and reference electrodes, respectively. The working electrode was a glassy carbon electrode (GCE, 3 mm in diameter) coated with 8 µL of catalyst ink. This ink was fabricated by ultrasonically dispersing 4 mg of catalyst in a solution containing 700 µL deionized water, 270 µL ethanol, and 30 µL of a 5 wt% Nafion solution. All measured potentials against the HgO/Hg reference were converted to the reversible hydrogen electrode (RHE) scale using the following equation:

$$E_{vs\ RHE} = E_{vs\ HgO/Hg} + E^{\theta}_{HgO/Hg}(0.0978\ V) + 0.0592\ pH$$

Where $E_{vs\,RHE}$ signifies the potential versus the RHE, $E_{vs\,HgO/Hg}$ is the potential relative to HgO/Hg electrode, $E^{\theta}_{HgO/Hg}$ implies the standard electrode potential of HgO/Hg electrode.

Linear sweep voltammetry (LSV) polarization curves were recorded in 1.0 M KOH at a scan rate of 5 mV s^{-1} with iR compensation. The corresponding Tafel slopes were then derived by fitting the polarization data to the Tafel equation:

$$\eta = a + b \log j$$

where η means overpotential of catalyst, a stands for intercept, b represents Tafel slope, and j represents the current density.

Electrochemical impedance spectroscopy (EIS) measurements were conducted over a frequency range of 0.1 to 100 kHz. To evaluate the electrochemical active surface area (ECSA), the electrochemical double-layer capacitance (C_{dl}) was determined. This was derived from cyclic voltammetry (CV) scans recorded at various scan rates (20, 30, 40, 50, and 60 mV s^{-1}) in the non-faradaic region.

The active site densities of the Ru-based catalysts were characterized by copper underpotential deposition (Cu_{UPD}). The experiments were performed in a solution containing 0.5 M H_2SO_4 and 5 mM $CuSO_4$. Prior to Cu_{UPD}, the working electrode was first cycled by cyclic voltammetry in a pure 0.5 M H_2SO_4 solution at a scan rate of 10 mV s^{-1}. Subsequently, the electrode was transferred to the $CuSO_4$-containing electrolyte and polarized at constant potentials of 0.220, 0.215, 0.210, 0.205, 0.200, 0.195 and 0.190 V (vs. RHE) for 100 s each to form a submonolayer of copper. The number of active sites (n) and the mass-based active site density (MSD) were then determined from the stripping charge (Q) of the deposited copper ($Cu_{UPD} \rightarrow Cu^{2+} + 2e^-$) using the following equation:

$$n = Q / 2F$$

$$MSD = n / m$$

Where F is the Faraday constant (96500 C mol^{-1}), m represents the mass of catalysts.

Supplementary Figures

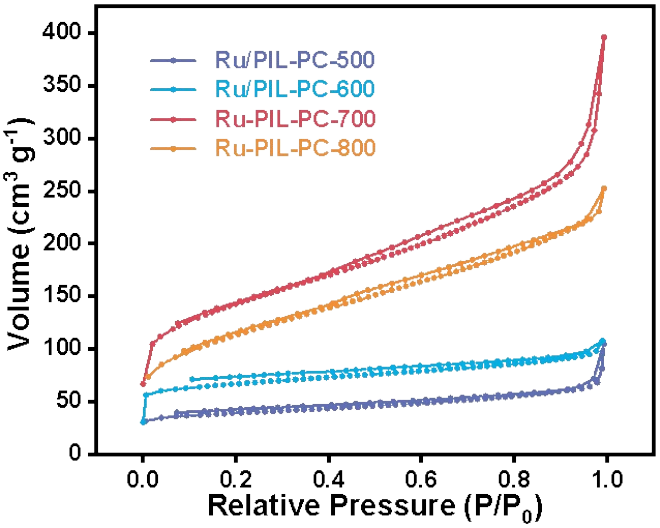

Fig. S1 N_2 adsorption/desorption isotherms of Ru/PIL-PC-T.

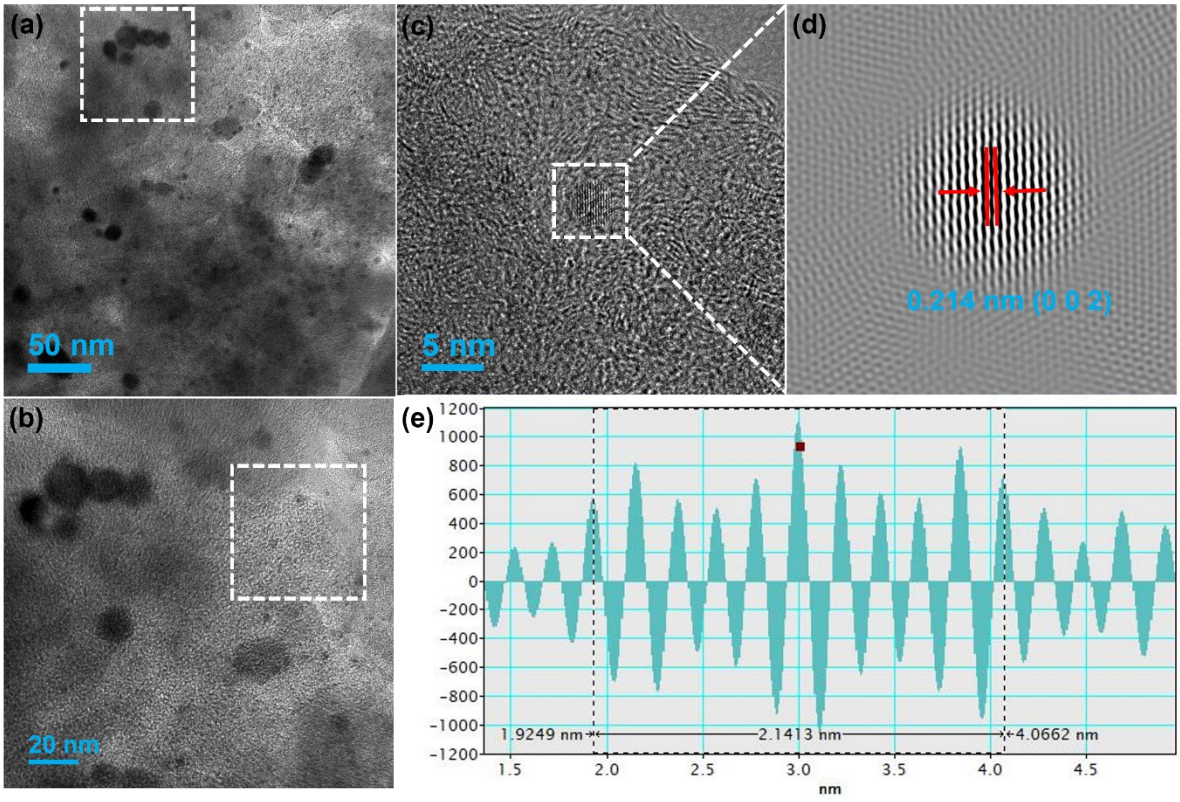

Fig. S2 TEM images (a,b) and HR-TEM images (c-e) of Ru@AC.

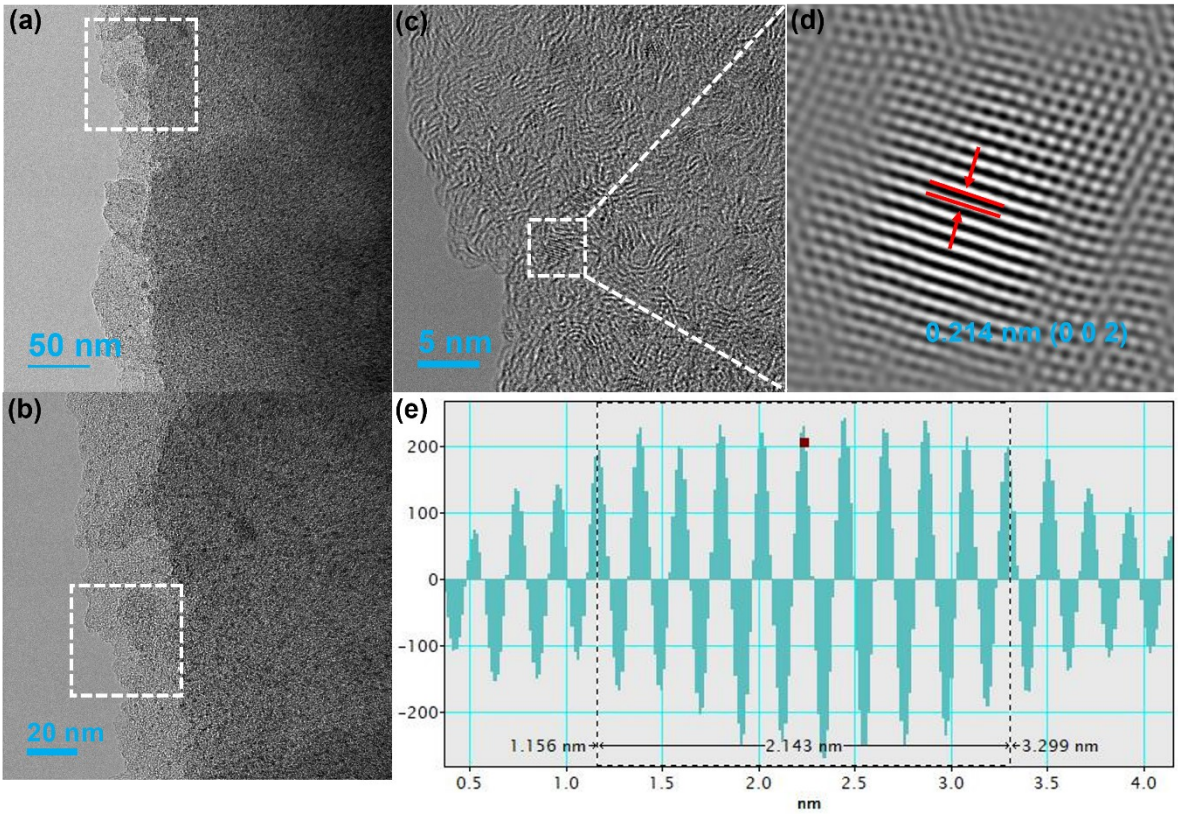

Fig. S3 TEM images (a,b) and HR-TEM images (c-e) of Ru/r-PILC.

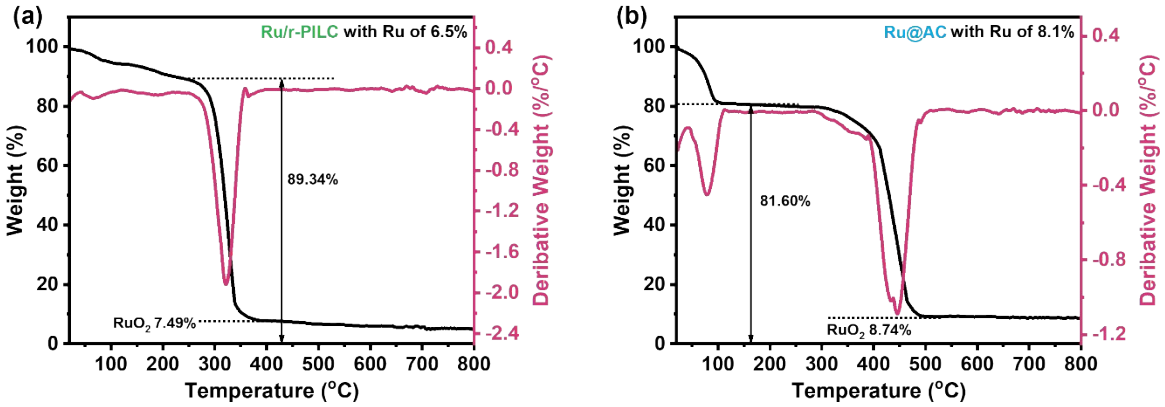

Fig. S4 TG and DTG curves of (a) Ru/r-PILC and (b) Ru@AC under air atmosphere.

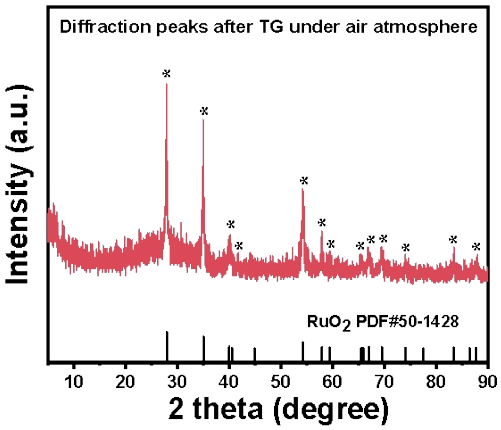

Fig. S5 Diffraction peaks of the samples after TG measurement under air atmosphere.

XRD analysis of Ru/PIL-PC-700, Ru/r-PILC and Ru@AC after TG measurement under air atmosphere all revealed the diffraction peaks of RuO_2, the TG content of Ru for each sample was calculated by converting the mass of RuO_2 to Ru and dividing it by the dry weight of the sample before thermal decomposition.

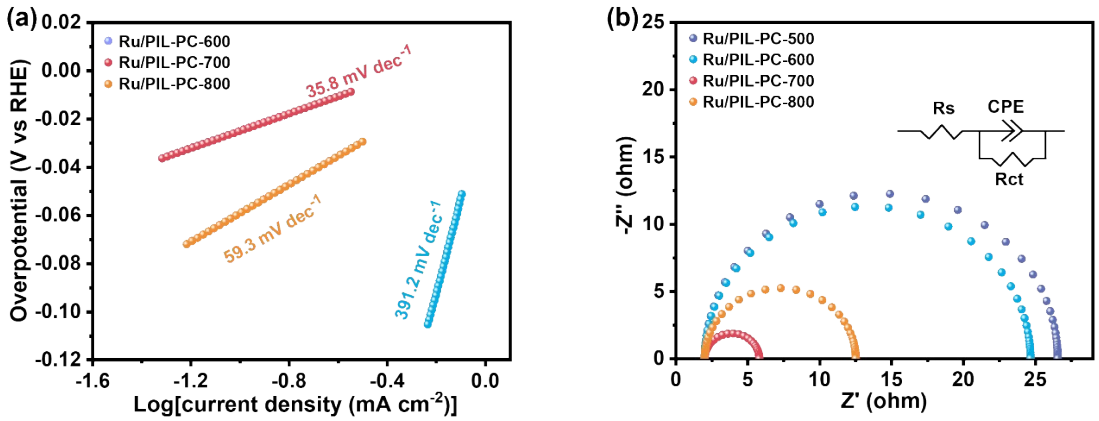

Fig. S6 (a) Tafel plots and (b) electrochemical impedance spectra of Ru/PIL-PC-500, Ru/PIL-PC-600, Ru/PIL-PC-700 and Ru/PIL-PC-800.

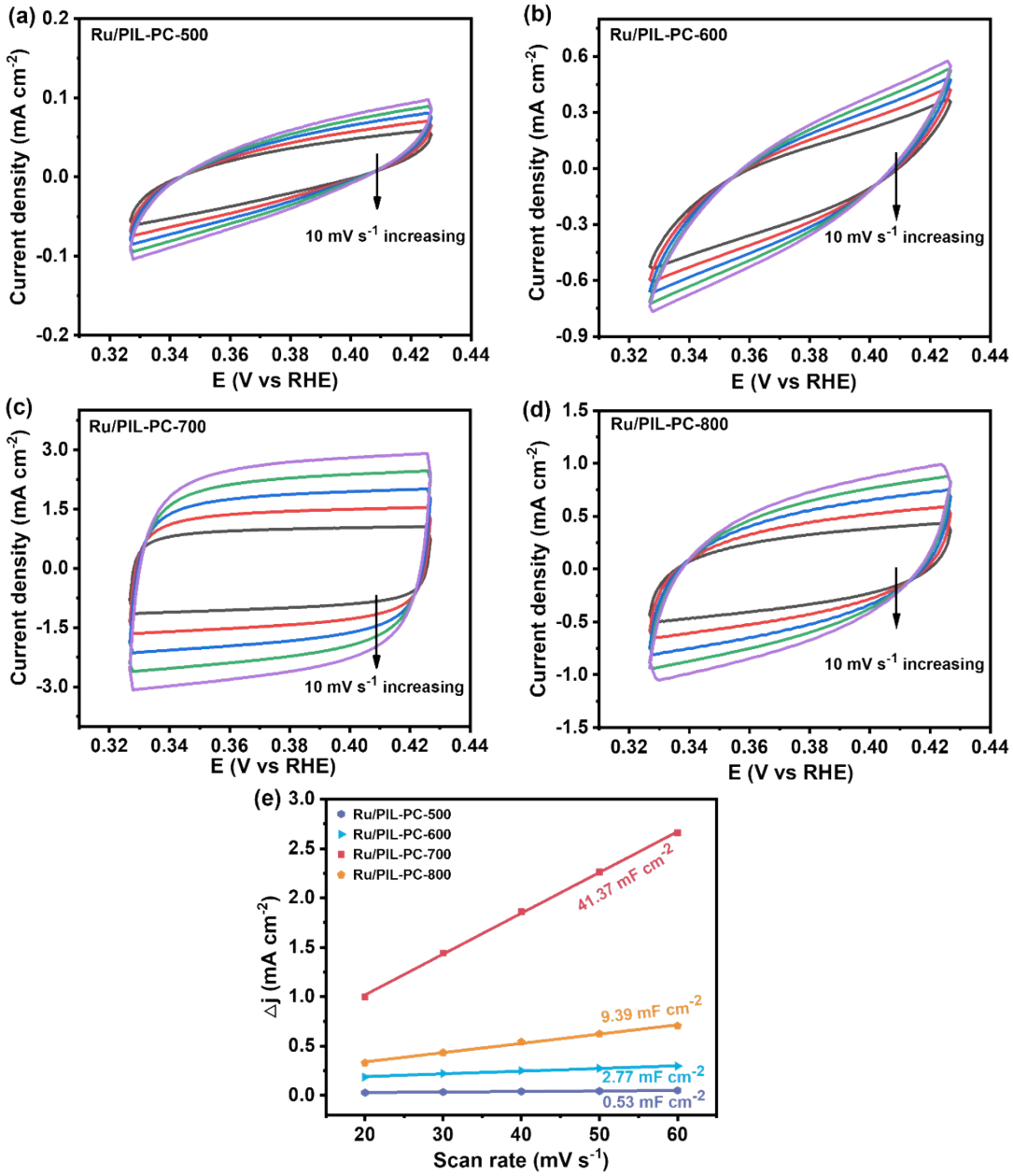

Fig. S7 CV curves of (a) Ru/PIL-PC-500, (b) Ru/PIL-PC-600, (c) Ru/PIL-PC-700 (d) Ru/PIL-PC-800 catalysts at the scan rate of 20, 30, 40, 50, 60 mV s^{-1} in 1 M KOH solution; (d) The corresponding C_{dl} calculated by linear fitting of the capacitive currents at 0.38V *vs.* scan rates.

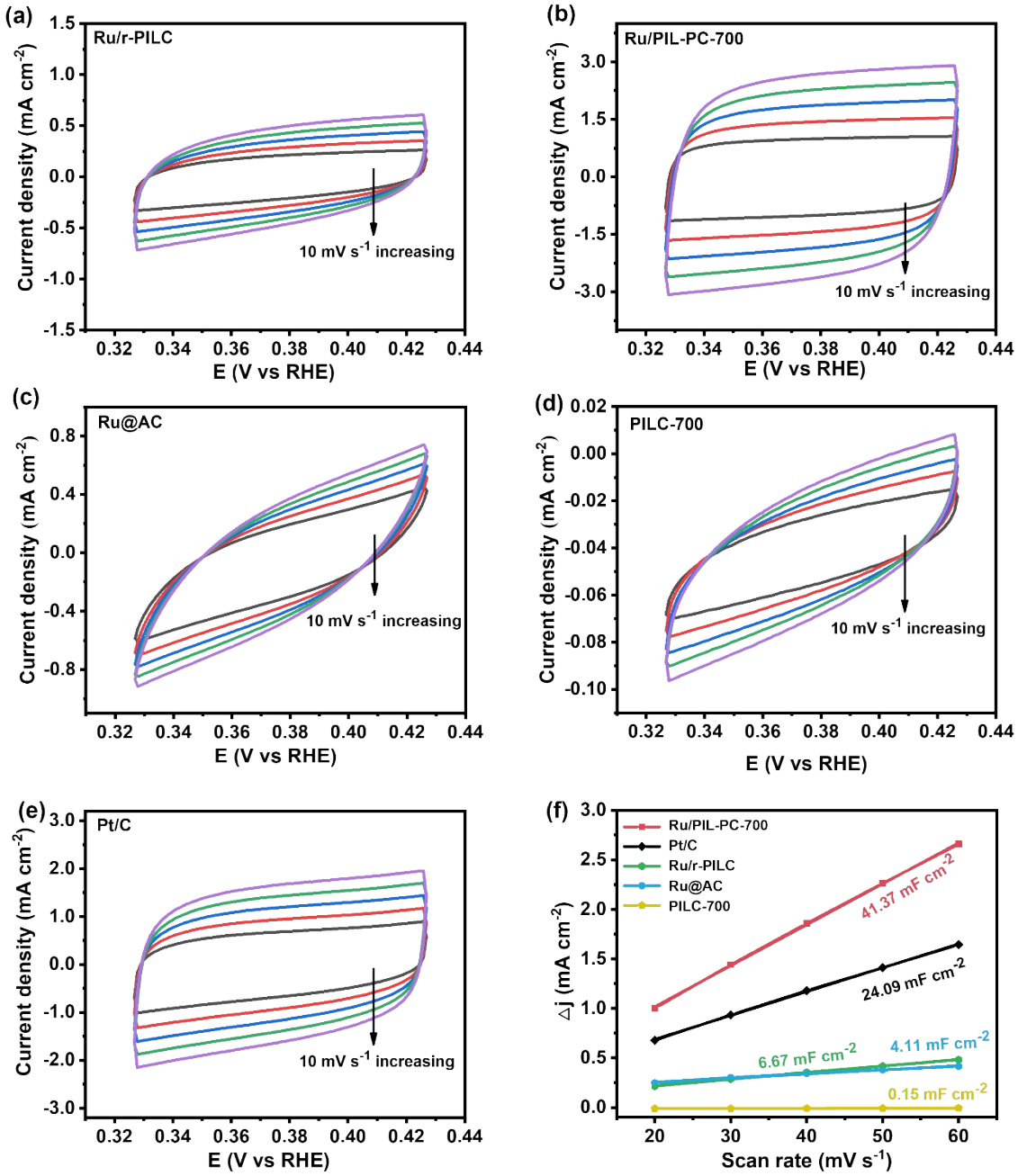

Fig. S8 CV curves of (a) Ru/r-PILC, (b) Ru/PIL-PC-700, (c) Ru@AC, (d) PILC-700, (e) Pt/C catalysts at the scan rate of 20, 30, 40, 50, 60 mV s^{-1} in 1 M KOH solution; (f) The corresponding C_{dl} calculated by linear fitting of the capacitive currents at 0.38V *vs.* scan rates.

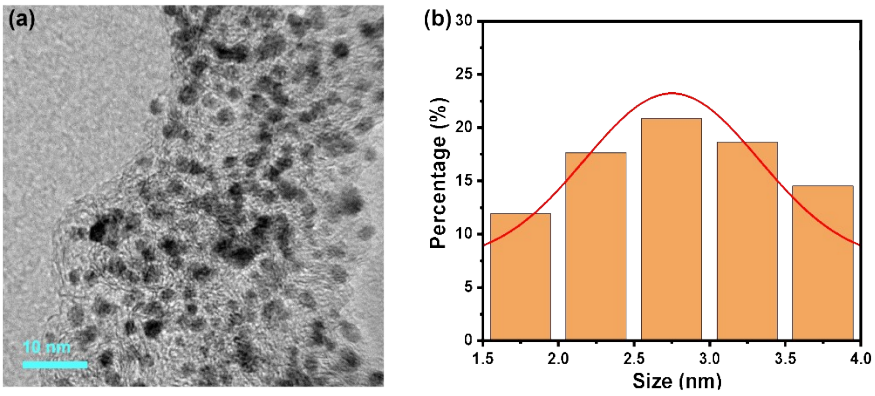

Fig. S9 (a) TEM image of commercial Pt/C, (b) the corresponding size distribution of Pt nanoparticles.

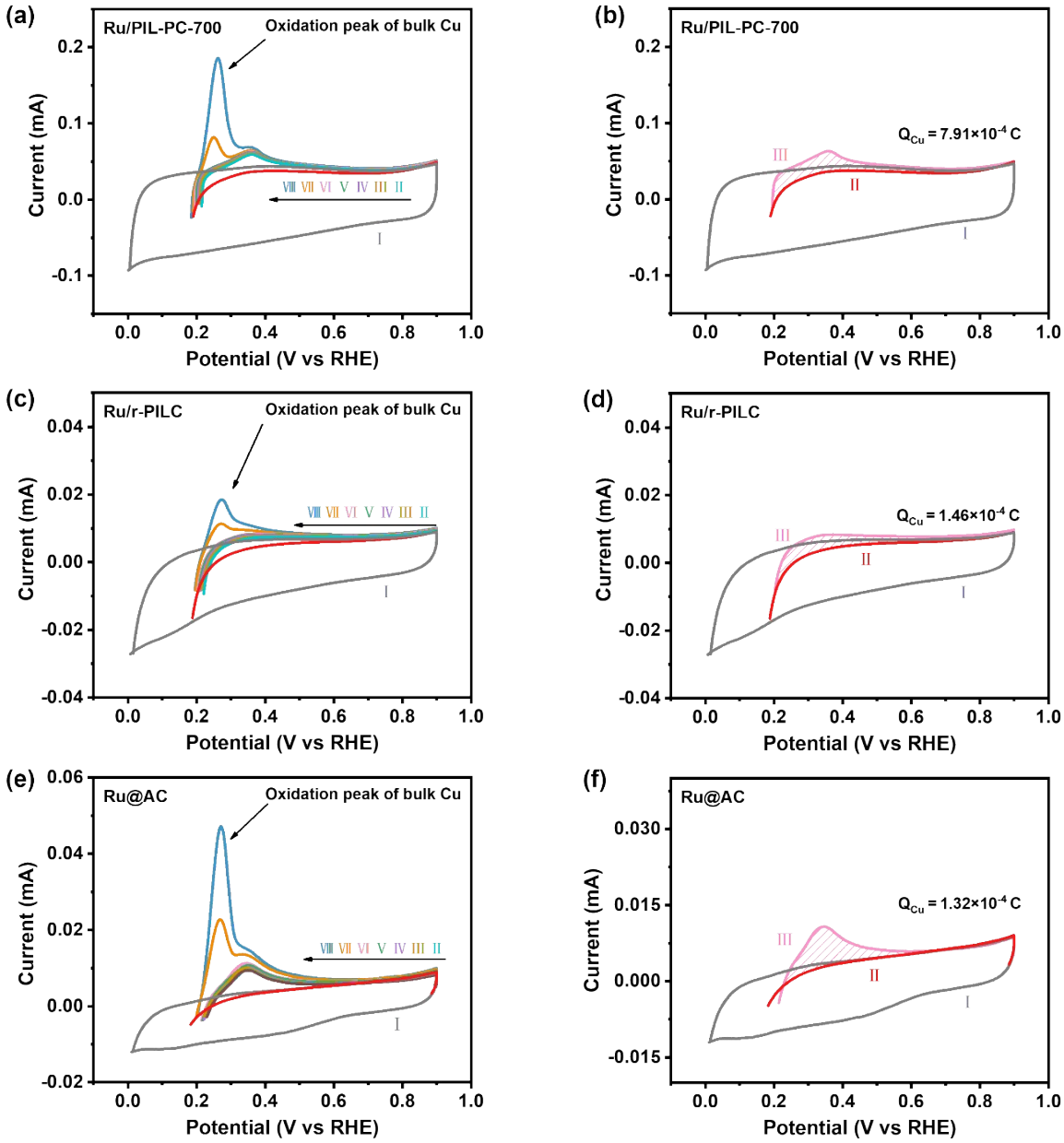

Fig. S10 Copper UPD in 0.5 M H_2SO_4 in the (I) absence and (II~VIII) presence of 5 mM $CuSO_4$ on (a) Ru/PIL-PC-700, (c) Ru/r-PILC and (e) Ru@AC, respectively. For II~VIII, the electrode was polarized at 0.185, 0.190, 0.195, 0.200, 0.205, 0.210 and 0.215 V for 100 s to form the UPD layers on Ru/PIL-PC-700, 0.190, 0.195, 0.200, 0.205, 0.210, 0.215 and 0.220 V for 100 s to form the UPD layers on Ru/r-PILC, and 0.180, 0.185, 0.190, 0.195, 0.200, 0.205 and 0.210 V for 100 s to form the UPD layers on Ru/r-PILC, respectively. Copper UPD in 0.5 M H_2SO_4 in the (I, II) absence and (III) presence of 5 mM $CuSO_4$ on (b) Ru/PIL-PC-700, (d) Ru/r-PILC and (f) Ru@AC. For II and III, the electrode was polarized at (b) 0.195 V, (d) 0.200 V and (f) 0.190 V for 100 s to form the UPD layer.

[

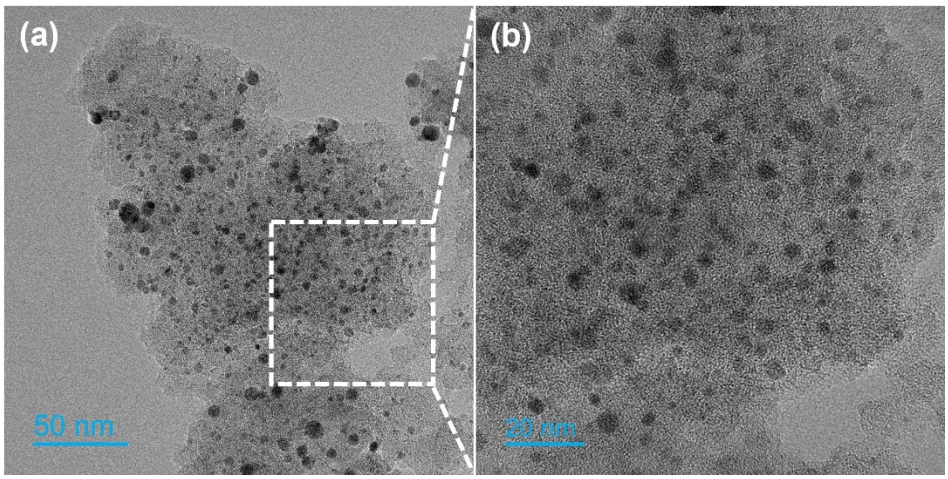

Fig. S11 TEM images of Ru/PIL-PC-700 after recycling.

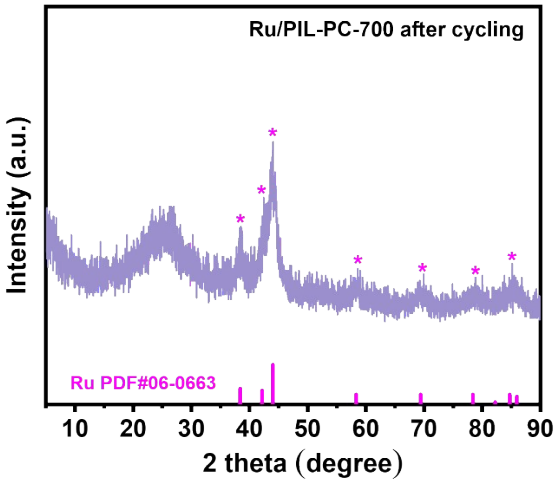

Fig. S12 XRD pattern of Ru/PIL-PC-700 after recycling.

Supplementary Tables

Table S1 Performance comparison of state-of-the-art electrocatalysts for the hydrogen evolution reaction in 1.0 M KOH.

Catalysts	Overpotential at 10 mA cm^{-2} (mV)	Tafel slope (mV dec^{-1})	Durability (cycle)	Reference
Ru/PIL-PC-700	23	35.8	10000	this work
Pt/C (Benchmark)	24~35	36~45	5000	ACS Nano 2022, 16, 7993−8004; Adv. Mater. 2024, 36, 2400433; Adv. Funct. Mater. 2024, 34, 2411081
Pt_{SA}-Mn_3O_4	24	54	N.A.[a]	Energy Environ. Sci. 2022, 15, 4592–4600
S-IrP_2@CNT	18.5	29.2	20000	ACS Catal. 2024, 14, 15015−15024
IrMo-CBC	12	28.06	3000	J. Am. Chem. Soc. 2023, 145, 16548−16556
Pt/C_{60}	25	55	3000	Nat. Commun. 2023, 14, 2460
$Pt_{1.15wt\%}$-Mo_2C/NCH	40	41.4	N.A.	Adv. Funct. Mater. 2025, e23916
ld-Ru@a-Co/Ti	33.5	39.6	N.A.	Chem. Commun. 2022, 58, 13588–13591
Fe-Mo_2C@NCF	65	76	1000	J. Mater. Chem. A 2020, 8, 19879
$CdNNi_3$	167	40	1000	Adv. Mater. 2025, 37, 2504607
CoP@Ni_2P Fe_2P	42	64	2000	Appl. Catal. B-Environ. 2023, 338, 123016
NFM-OV_R/NF	25	46.9	5000	Adv. Mater. 2024, 36, 2411134

[a] N. A. = Not available.

Table S2 BET surface area and pore volume of different catalysts.

Catalyst	S_{BET} (m^2 g^{-1})
Ru/PIL-PC-500	122.5
Ru/PIL-PC-600	207.5
Ru/PIL-PC-700	476.3
Ru/PIL-PC-800	391.2

Table S3 XPS data for the content and distribution of C 1s of different catalysts.

Catalyst	Concentration of different C speices / %			
	sp^2 C (284.8 eV)	sp^3 C (285.3 eV)	C-N/O (286.5 eV)	C=N/O (288.2 eV)
Ru/r-PILC	50.3	23.6	21.3	4.8
Ru/PIL-PC-700	47.2	26.9	21.2	4.7
Ru@AC	50.9	29.7	15.4	4.0

Table S4 XPS data for the surface species of different catalysts.

Catalyst	Atomic/ weight percentages of surface elements (%)			
	C (at.% / wt.%)	N (at.% / wt.%)	O (at.% / wt.%)	Ru (at.% / wt.%)
Ru/r-PILC	78.09 / 69.79	5.10 / 5.32	16.04 / 19.10	0.77 / 5.79
Ru/PIL-PC-700	83.37 / 73.46	4.56 / 4.69	10.84 / 12.73	1.23 / 9.12
Ru@AC	87.40 / 79.55	1.22 / 1.30	10.55 / 12.79	0.83 / 6.36

The atomic percentage (at%) measured by XPS is converted into the weight percentage (wt%) by following equation:

$$x\,wt\% = \frac{M_x \times x\,(at\%)}{12.01 \times C\,(at\%) + 14.01 \times N\,(at\%) + 16.00 \times O\,(at\%) + 101.07 \times Ru\,(at\%)}$$

Where 12.01, 14.01, 16.00, and 101.07 are the atomic mass of C, N, O and Ru, respectively.

Table S5 Comparison of HER performance of Ru NPs ever reported in 1.0 M KOH.

Catalysts	Overpotential at 10 mA cm^{-2} (mV)	Tafel slope (mV dec^{-1})	Durability (cycle)	Reference
Ru/PIL-PC-700	23	35.8	10000	this work
Ru/Zn-N-C	17.6	44.29	5000	Adv. Mater. 2024, 36, 2308798
BaRuO3	26	26	N.A.	J. Am. Chem. Soc. doi.org/10.1021/jacs.5c16183
Ru-NBC	27	38.15	N.A.	ACS Nano 2025, 19, 7948−7961
Ru SA/Co_3O_4	44	57	N.A.	ACS Nano 2025, 19, 11176−11186
Ru_3/OCNT	19	25.63	N.A.	Adv. Funct. Mater. 2025, 35, 2503678
Ru-RuO_2/C	31	85.4	N.A.	Adv. Sci. 2025, 12, 2414534
Fcc RuFe@fcc Ru	17	14.5	1000	Nano Lett. 2025, 25, 9872−9879
Ru-Mo_2C@CNT	15	26	10000	Nat. Commun. 2021, 12, 4018
homo-PIL-Ru/C-600	16	42	10000	Small Methods 2021, 5, 2100505
Ru@GNs	40	28	1000	Carbon 2020, 166, 388−395
Ru/PC	21	46.6	1000	Green Chem. 2020, 22, 835−842
Ru@SC-CDs	29	57	5000	Nano Energy 2019, 65, 104023
Ru@CN	32	53	2000	Energy Environ. Sci. 2018, 11, 800−806

Ru/Co-N-C	23	27.8	N.A.	Adv. Mater. 2022, 34, 2110103
Ru@NCN	36	37	5000	J. Mater. Chem. A 2021, 9, 13958−13966
Ru_{40}@mONC	28	25	3000	Nano Res. 2022, 15, 5134−5142
V_O-Ru/HfO_2-OP	39	22	5000	Nat. Commun. 2022, 13, 1270
Ru@NC	25	29	N.A.	Adv. Mater. 2023, 35, 2301133
Ru/C_3N_4/C [a]	79	N. A. [b]	1000	J. Am. Chem. Soc. 2016, 138, 16174

[a] The electrolyte is 0.1 M KOH. [b] N. A. = Not available.